Monthly Notices
of the
ROYAL ASTRONOMICAL SOCIETY

MNRAS **456,** L35–L39 (2016) doi:10.1093/mnrasl/slv174

No direct coupling between bending of galaxy disc stellar age and light profiles

T. Ruiz-Lara,[1,2]★ I. Pérez,[1,2] E. Florido,[1,2] P. Sánchez-Blázquez,[3] J. Méndez-Abreu,[4] M. Lyubenova,[5] J. Falcón-Barroso,[6,7] L. Sánchez-Menguiano,[1,8] S. F. Sánchez,[9] L. Galbany,[10,11] R. García-Benito,[8] R. M. González Delgado,[8] B. Husemann,[12] C. Kehrig,[8] Ángel R. López-Sánchez,[13,14] R. A. Marino,[15,16] D. Mast,[17,18] P. Papaderos,[19] G. van de Ven,[20] C. J. Walcher,[21] S. Zibetti[22] and the CALIFA team

Affiliations are listed at the end of the paper

Accepted 2015 October 29. Received 2015 October 26; in original form 2015 October 1

ABSTRACT

We study the stellar properties of 44 face-on spiral galaxies from the Calar Alto Legacy Integral Field Area survey via full spectrum fitting techniques. We compare the age profiles with the surface brightness distribution in order to highlight differences between profile types (type I, exponential profile; and II, down-bending profile). We observe an upturn ('U-shape') in the age profiles for 17 out of these 44 galaxies with reliable stellar information up to their outer parts. This 'U-shape' is not a unique feature for type II galaxies but can be observed in type I as well. These findings suggest that the mechanisms shaping the surface brightness and stellar population distributions are not directly coupled. This upturn in age is only observable in the light-weighted profiles while it flattens out in the mass-weighted profiles. Given recent results on the outer parts of nearby systems and the results presented in this Letter, one of the most plausible explanations for the age upturn is an early formation of the entire disc (∼10 Gyr ago) followed by an inside-out quenching of the star formation.

Key words: techniques: spectroscopic – galaxies: evolution – galaxies: formation – galaxies: spiral – galaxies: stellar content – galaxies: structure.

1 INTRODUCTION

The long dynamical time-scales displayed by the stars populating the outer and low surface brightness (SB) regions of disc galaxies make the study of these regions a key element in the understanding of galaxy formation and evolution. Pioneering studies on the light distribution of spiral galaxies found an exponential decline with radius (e.g. Freeman 1970). However, deeper and higher quality images allow us to reach further out. Nowadays, we know that disc galaxies present a wide variety of shapes in the SB profiles of their outer parts (Erwin, Beckman & Pohlen 2005; Pohlen & Trujillo 2006) showing a continuation of the inner exponential behaviour (type I; e.g. Bland-Hawthorn et al. 2005), a lack of light (type II) or an excess of light (type III). Some of the proposed scenarios for the origin of these profiles include a maximum in the angular momentum of the baryonic matter (van der Kruit 1987), a star formation (SF) threshold (Kennicutt 1989; Schaye 2004), or a combination of both (van den Bosch 2001). However, a conclusive explanation is still missing.

Recent theoretical works claim that a substantial number of stars move from their birth location (e.g. Battaner, Florido & Jiménez-Vicente 2002; Sellwood & Binney 2002; Minchev et al. 2012). This radial migration has implications on the outer parts of type II galaxies. Roškar et al. (2008), through isolated disc simulations, found that outward-migrated stars are the main population in the external parts of disc galaxies as its outer gas surface density is well below the threshold for SF. This change in the stellar populations is responsible for a break in the mass distribution and produces an upturn in the age profile ('U-shape' age profiles). Cosmological simulations are needed to assess the effect of the environment and satellite accretion in shaping these outer discs (Younger et al. 2007; Bird, Kazantzidis & Weinberg 2012). Sánchez-Blázquez et al. (2009), analysing cosmological simulations, did not find any break in the mass distribution. Even more, the 'U-shape' age profile was recovered even when radial migration was not allowed. They concluded

★ E-mail: ruizlara@ugr.es

that the outer ageing of the stellar populations must be due to a radial change in the SF rate caused by a drop in the gas density. Theoretical models for type I and III galaxies are less elaborated and thus, no clear predictions have been stated so far. The analysis of the stellar content in these low-density regions in real galaxies is key to refine and constrain galaxy formation models.

Some observational works have studied the stellar content in the outer parts of spiral galaxies. Bakos, Trujillo & Pohlen (2008) stacked 85 $g - r$ colour profiles from Pohlen & Trujillo (2006) separating between type I, II, and III galaxies. They found a clear reddening in the outer parts of their type II galaxies while type I and type III galaxies showed a flattening or a slight blue upturn. This reddening has been also found regardless their SB in Roediger et al. (2012). To minimize the age–metallicity degeneracy that affects colour-based analysis, spectroscopic studies are needed. However, obtaining high-quality spectra to analyse the stellar content in these regions is not straightforward. Yoachim, Roškar & Debattista (2012), using integral field spectroscopy (IFS) data, examined the radial stellar content of 12 spiral galaxies integrating over elliptical apertures. They were able to reach the outer parts for six type II discs but just three of them displayed the predicted age 'U-shape' (light-weighted values). This 'U-shape' implies the presence of old stellar populations in these outer parts regardless of the physical interpretation for such shape.

There is evidence of the existence of this old outer disc from the analysis of individual stars in very nearby systems (e.g. Bernard et al. 2012, 2015; Radburn-Smith et al. 2012). In addition, recent studies have observed such behaviour for galactic systems regardless of their morphology, formation, or mass. Zhang et al. (2012) analysed 34 dwarf irregular galaxies finding hints of old stellar populations over the entire disc from their spectral energy distribution (SED) modelling. Similar results have been found by Zheng et al. (2015), analysing SED modelling of 698 galaxies from the Pan-STARRS1 Medium Deep Survey images.

To date, there are no clear observational evidences of a correlation between SB and other stellar parameters such as age. Here, we present for the first time the radial behaviour of the age of the stellar populations [light- and mass-weighted (M-W)] up to the outer parts of a large sample of spiral galaxies from the Calar Alto Legacy Integral Field Area survey (CALIFA; Sánchez et al. 2012a), focusing on the relation between the age distribution in the outer parts and their SB profiles.

2 SAMPLE AND CALIFA DATA

In this work, we make use of the IFS data from the CALIFA survey (Sánchez et al. 2012a). CALIFA data were obtained at the 3.5 m telescope at Calar Alto using the PMAS/PPAK spectrograph. This project provides high-quality spectra over a wide field-of-view (FoV) of 72 arcsec × 64 arcsec of ∼600 galaxies in the local Universe (Walcher et al. 2014) with two different observing set-ups: one at higher resolution (V1200); and the other at a lower resolution (V500). The wavelength range of the V500 (V1200) data is 3745–7500 Å (3650–4840 Å) with a spectral resolution of full width at half-maximum (FWHM) = 6.0 Å (FWHM = 2.7 Å). For more information about the CALIFA data, see García-Benito et al. (2015). The wide FoV of the instrument and the thoroughly tested sky subtraction procedure implemented in the reduction pipeline allow us to analyse the stellar and gas content up to the outer parts (Husemann et al. 2013; Marino et al. 2015). We consider 'outer parts' of our galaxies, those beyond the break radius for type II and beyond three disc-scalelengths for type I. We use a combination of the V500 and the V1200 (degraded to the V500 resolution) data cubes (v1.5) in order to expand the wavelength range to 3700–7500 Å (COMBO cube).

We choose a subsample of 44 low-to-intermediate-inclined ($0^\circ \leq i \leq 75^\circ$), small ($d_{25} < 94.8$ arcsec), non-interacting spiral ($0 \leq T \leq 8$) galaxies observed by CALIFA based on the Hyperleda catalogue. Observational constraints such as high S/N in the outer parts or enough instrument FoV have been taken into account to ensure a reliable recovery of the stellar content up to the outer parts.

We have carefully analysed the two-dimensional light distribution in our galaxies to characterize their morphology and SB profiles. We use the fully calibrated Sloan Digital Sky Survey (SDSS) images (g, r, and i bands) from the seventh data release (DR7; Abazajian et al. 2009) and the GASP2D software (GAlaxy Surface Photometry 2 Dimensional Decomposition; Méndez-Abreu et al. 2008). GASP2D adopts a pixel-by-pixel Levenberg–Marquardt algorithm to fit the two-dimensional SB distribution of the galaxy allowing us to model different structural galaxy components such as bulge, disc (broken disc), or bar. All this two-dimensional analysis will be presented in detail in Méndez-Abreu et al. (in preparation).

3 ANALYSIS

In this section, we describe the procedure followed to analyse the stellar content from the CALIFA data. A complete description of the analysis and the sample of galaxies will be given in Ruiz-Lara et al. (in preparation).

(i) We apply a stellar kinematic extraction method designed for dealing with CALIFA data (Falcón-Barroso et al., in preparation) to correct the observed data cubes for the stellar kinematics effect. After applying an adaptive Voronoi method following Cappellari & Copin (2003) with a goal S/N of 20 and considering only spaxels with continuum S/N > 3, we use the penalized pixel fitting code (PPXF; Cappellari & Emsellem 2004; Cappellari et al. 2011) to extract the stellar kinematics.

(ii) We perform a radial elliptical binning to the kinematic-corrected data (rest frame and a common velocity dispersion). We use different steps from one ellipse to the next in order to reach an S/N > 20 in the spectra (per Å). The centre, ellipticity, and position angle of the ellipses are fixed, matching the outer disc isophotes.

(iii) We use GANDALF (Gas AND Absorption Line Fitting; Falcón-Barroso et al. 2006; Sarzi et al. 2006) to subtract the emission line component from the observed spectra. We adopt an optimal subset of the Vazdekis et al. (2010) models (hereafter MILES models) as stellar templates. We use 30 log-spaced age bins (from 0.063 to 17.8 Gyr) and all MILES metallicities.

(iv) The stellar population parameters are derived using STEllar Content and Kinematics via Maximum A Posteriori likelihood (STECKMAP; Ocvirk et al. 2006a,b). STECKMAP is aimed at simultaneously recovering the stellar content and kinematics using a Bayesian method via a maximum a posteriori algorithm. It is based on the minimization of a penalized χ^2 while no a priori shape of the solution is assumed (i.e. it is a non-parametric code). See Sánchez-Blázquez et al. (2011, 2014) for further details. To compute the age, luminosity, or M-W (Q–W), we use the following equation:

$$\langle \log(\mathrm{Age[yr]}) \rangle_{\mathrm{Q-W}} = \frac{\sum_i Q(i) * \log(\mathrm{Age}_i)}{\sum_i Q(i)}, \quad (1)$$

where $Q(i)$ is the light or mass fraction of each age bin (i). We fix the stellar kinematics in order to avoid the velocity dispersion–metallicity degeneracy (Sánchez-Blázquez et al. 2011). Statistical

Table 1. List of galaxies displaying 'U-shape' age profiles. (1) Name of the galaxy; (2) right ascension (J2000); (3) declination (J2000); (4) morphological type; (5) bar (1, yes; 0, no); (6) surface brightness profile type; (7) inner disc scalelength (h_{in} in kpc); (8) outer disc scalelength (h_{out} in kpc); (9) break radius (R_{break}) in units of h_{in}; (10) minimum age position (R_{min} in kpc). Columns (1)–(4) from the hyperleda data base. Columns (5)–(9) from our 2D decomposition.

Galaxy	RA (^{h}:^{m}:^{s})	Dec. ($^\circ$ ′ ″)	Morphological type	Bar (1, yes; 0 no)	SB profile	h_{in} (kpc)	h_{out} (kpc)	R_{break}/h_{in}	R_{min} (kpc)
(1)	(2)	(3)	(4)	(5)	(6)	(7)	(8)	(9)	(10)
IC1199	16:10:34.34	+10:02:25.32	Sbc	0	II	5.83	2.54	1.46	7.00
NGC 0234	00:43:32.39	+14:20:33.24	SABc	0	II	5.56	3.11	1.55	6.67
NGC 0551	01:27:40.63	+37:10:58.73	SBbc	1	I	5.09	–	–	10.18
NGC 2449	07:47:20.29	+26:55:48.70	Sab	1	I	4.50	–	–	6.53
NGC 2572	08:21:24.62	+19:08:51.99	Sa	1	I	4.79	–	–	8.62
NGC 3815	11:41:39.29	+24:48:01.79	Sab	1	I	2.83	–	–	7.36
NGC 4470	12:29:37.77	+07:49:27.12	Sa	0	I	1.76	–	–	2.20
NGC 4711	12:48:45.86	+35:19:57.72	SBb	0	II	3.94	2.39	1.85	6.42
NGC 5376	13:55:16.05	+59:30:23.80	SABa	0	II	2.95	1.69	1.50	3.54
NGC 5633	14:27:28.38	+46:08:47.67	Sb	0	I	1.43	–	–	2.43
NGC 5732	14:40:38.95	+38:38:16.16	Sbc	0	II	2.58	1.50	3.75	3.61
NGC 6155	16:26:08.33	+48:22:00.46	Sc	0	II	1.95	1.22	3.27	3.02
NGC 6478	17:48:37.73	+51:09:13.68	Sc	0	II	9.57	5.50	1.31	15.31
NGC 7311	22:34:06.79	+05:34:13.16	Sab	0	I	3.63	–	–	7.44
NGC 7321	22:36:28.02	+21:37:18.35	Sbc	1	II	44.69	4.95	0.32	12.07
UGC00036	00:05:13.88	+06:46:19.30	Sa	1	I	4.08	–	–	8.57
UGC05396	10:01:40.48	+10:45:23.13	Sc	1	II	6.38	2.65	2.67	10.85

errors are computed by means of 25 Monte Carlo simulations as computed by STECKMAP. Once STECKMAP has determined the best combination of model templates (Vazdekis et al. 2010) to fit the observed spectrum, we add noise based on the spectrum S/N and run STECKMAP again. This test is done 25 times and the standard deviation of the recovered age is considered as the error. Along with the age profiles, metallicity profiles are obtained. We must warn the reader that although we have extensively tested our method (Ruiz-Lara et al. 2015) against the well-known age–metallicity degeneracy using Monte Carlo (MC) simulations finding no clear trends, some effects might still remain.

4 RESULTS AND DISCUSSION

We study the radial distribution of stellar parameters up to the outer parts (i.e. galaxies for which we reach beyond their break radius or at least $\sim$ 3 disc-scalelengths) and relate these properties to their SB profiles for a sample of 44 galaxies (see Section 2). Our selection criteria leave us with no galaxies displaying a type III SB profile, so our results are statistically limited to type I and II galaxies.

We find that 17 galaxies (8 type I and 9 type II galaxies), i.e. 39 per cent (40 per cent of the type I and 38 per cent of the type II galaxies) of our final sample show clear 'U-shapes' in the luminosity-weighted (L-W) age profile regardless their SB distribution (Table 1). Such 'U-shape' disappears for all cases when the age is M-W, displaying a flat distribution in the whole disc ($\sim$10 Gyr) with a slight correlation with morphological type in the sense of what found in González Delgado et al. (2015) but to a lesser degree. The remaining 27 galaxies present different behaviours with no clear pattern. Fig. 1 shows the age profiles for two galaxies as examples of a type I (NGC 0551) and a type II (NGC 4711).

For the first time, 'U-shaped' age profiles are found indistinctly in type I and II galaxies from spectroscopic data. To date, such profiles have been found (observationally and theoretically) just in type II galaxies (Bakos et al. 2008; Roškar et al. 2008; Sánchez-Blázquez et al. 2009; Yoachim et al. 2012). However, recent cosmological simulations (Ruiz-Lara et al., submitted) analysing 19 Milky Way-like galaxies with different SB profiles from the Ramses Disk Environment Study (RaDES) set of galaxies (Few et al. 2012) show this upturn in age for all of them (in agreement with Minchev et al. 2015). An important result from this work in constraining galaxy formation models is the fact that not all the analysed galaxies display a 'U-shape' in the age profile and it appears in both type I and II. These findings allow us to conclude that the mechanisms responsible for shaping the SB distribution are not coupled to those shaping the stellar age profile. Thus, we can rule out that breaks are linked to particular changes in the stellar populations. In other words, old outer discs do not lead to type II SB profiles as proposed by numerical simulations. Other aspects must be responsible for the observed SB profiles (e.g. Herpich et al. 2015).

It is important to note that the 'U-shape' age profiles shown in simulations are M-W quantities. However, our M-W profiles show no sign of 'U-shape' at all, meaning that SF in simulations has been higher at later times than in real galaxies. We also tested if there is any correlation between the 'U-shape' occurrence with morphology, galaxy mass, and bar presence. We do not find any pattern among these properties, although we suffer from low number statistics and these relations should be further investigated.

In most cases, the observed minimum age is located prior to the break radius, with the exceptions of NGC 6478 and NGC 4711. There is no consensus about a possible link between the location of the break in the light distribution and the minimum in age, neither from observations nor from theoretical works. While some works point towards younger stars (bluer colours) located exactly at the break radius (Bakos et al. 2008; Roškar et al. 2008; Marino et al. 2015) others claim that such minimum age is found prior to it (Sánchez-Blázquez et al. 2009; Yoachim et al. 2012) or with no relation at all (Roediger et al. 2012). From this work, we can rule out that the minimum in age is exactly located at the break radius.

L-W radial stellar age distributions (see example in left-hand panel of Fig. 2) for the 44 galaxies show clear evidences suggesting that SF in them have been quenched inside-out (i.e. inner

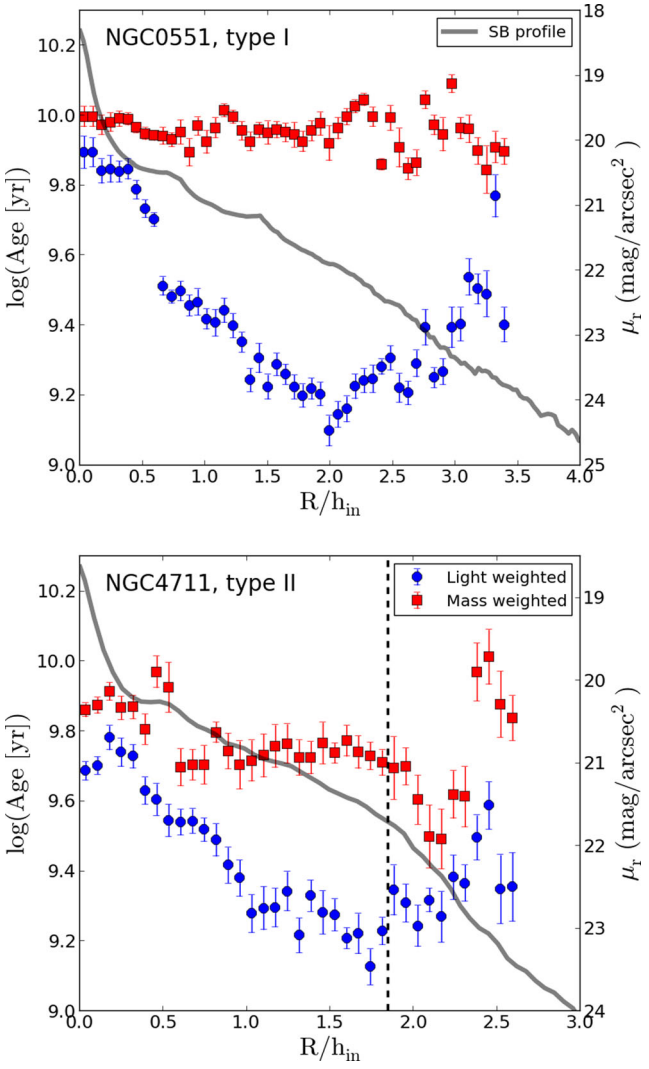

Figure 1. Age radial profile in logarithmic scale and surface brightness profile (SDSS *r*-band) for NGC 0551 (top panel, type I) and NGC 4711 (bottom panel, type II). Red (blue) squares (points) indicate mass-weighted (light-weighted) values. The black dashed line is located at the break radius. Grey continuous lines corresponds to the SB profiles (see right *y*-axis).

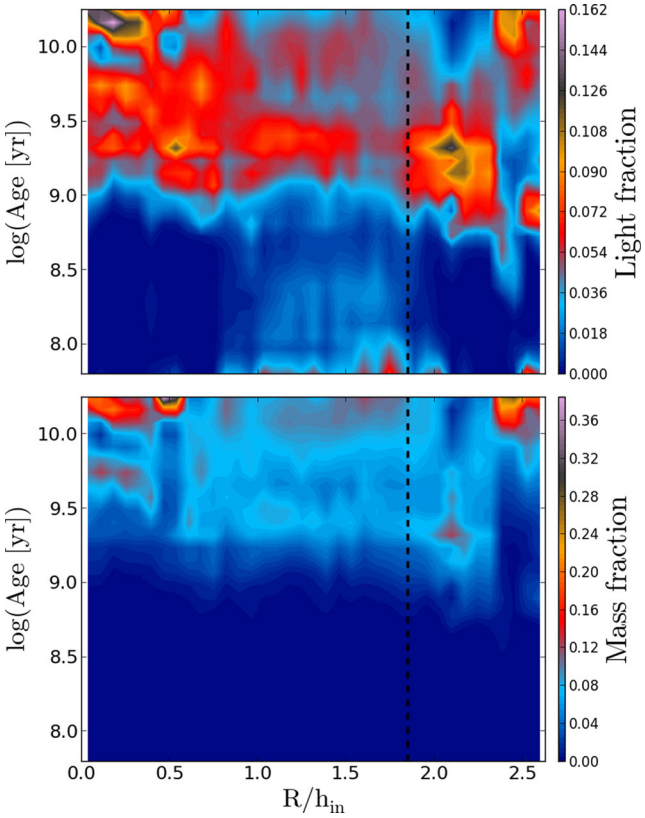

Figure 2. Radial stellar age distribution for NGC 4711: Upper panel, luminosity-weighted; bottom panel, mass-weighted. The black dashed line is located at the break radius.

regions mainly dominated by old stars, with young stars becoming more important as we move outwards), in agreement with previous CALIFA works on the stellar mass growth (Pérez et al. 2013), stellar populations radial profiles (González Delgado et al. 2014; Sánchez-Blázquez et al. 2014; González Delgado et al. 2015) and gas abundance gradients (Sánchez et al. 2012b, 2014, Sánchez-Menguiano et al., submitted). Apart from that, an outermost old stellar component appears again for those galaxies presenting 'U-shape'. The M-W radial stellar age distributions (see example in right-hand panel of Fig. 2) do not show any population younger than 2 Gyr with the bulk of stars being ∼10 Gyr old.

This work supports recent observations finding old outer discs (e.g. Bernard et al. 2012, 2015; Radburn-Smith et al. 2012), pointing towards an early SF along the entire disc followed by an inside-out SF quenching as the cause of the age upturn. However, we cannot rule out scenarios considering the effects of other mechanisms (radial migration, different SF recipes, satellite accretion, etc.) shaping different SB profiles after the age profile is built.

5 CONCLUSIONS

In this Letter, we study the stellar age profiles up to the outer parts of the discs of a large sample of galaxies selected from CALIFA. We conclude that (i) mechanisms shaping the SB and stellar distributions are not coupled, i.e. more processes must be involved in the type II SB profile formation; (ii) 'U-shape' age profiles are not unique for type II discs; (iii) this upturn is not a universal feature (appears only in 17 out of 44 galaxies). A possible explanation for the age upturn compatible with our results is an early build-up of the entire disc followed by an inside-out SF quenching.

ACKNOWLEDGEMENTS

This Letter is based on data from the CALIFA Survey (http://califa.caha.es), funded by the Spanish Ministry of Science (grant ICTS-2009-10), and the Centro Astronómico Hispano-Alemán. This research has been partly supported by the Spanish Ministry of Science and Innovation under grants AYA2011-24728, AYA2013-48226-C3-1-P and Consolider-Ingenio CSD2010-00064; and by the Junta de Andalucía (FQM-108). TRL thanks the support of the Spanish Ministerio de Educación, Cultura y Deporte (FPU fellowship). We acknowledge the usage of the HyperLeda data base (http://leda.univ-lyon1.fr) and SDSS data (http://www.sdss.org/collaboration/citing-sdss/).

REFERENCES

Abazajian K. N. et al., 2009, ApJS, 182, 543
Bakos J., Trujillo I., Pohlen M., 2008, ApJ, 683, L103

Battaner E., Florido E., Jiménez-Vicente J., 2002, A&A, 388, 213
Bernard E. J. et al., 2012, MNRAS, 420, 2625
Bernard E. J. et al., 2015, MNRAS, 446, 2789
Bird J. C., Kazantzidis S., Weinberg D. H., 2012, MNRAS, 420, 913
Bland-Hawthorn J., Vlajić M., Freeman K. C., Draine B. T., 2005, ApJ, 629, 239
Cappellari M., Copin Y., 2003, MNRAS, 342, 345
Cappellari M., Emsellem E., 2004, PASP, 116, 138
Cappellari M. et al., 2011, MNRAS, 413, 813
Erwin P., Beckman J. E., Pohlen M., 2005, ApJ, 626, L81
Falcón-Barroso J. et al., 2006, MNRAS, 369, 529
Few C. G., Gibson B. K., Courty S., Michel-Dansac L., Brook C. B., Stinson G. S., 2012, A&A, 547, A63
Freeman K. C., 1970, ApJ, 160, 811
García-Benito R. et al., 2015, A&A, 576, A135
González Delgado R. M. et al., 2014, A&A, 562, A47
González Delgado R. M. et al., 2015, A&A, 581, A103
Herpich J. et al., 2015, MNRAS, 448, L99
Husemann B. et al., 2013, A&A, 549, A87
Kennicutt R. C., Jr, 1989, ApJ, 344, 685
Marino R. A. et al., 2015, preprint (arXiv: e-prints)
Méndez-Abreu J., Aguerri J. A. L., Corsini E. M., Simonneau E., 2008, A&A, 478, 353
Minchev I., Famaey B., Quillen A. C., Di Matteo P., Combes F., Vlajić M., Erwin P., Bland-Hawthorn J., 2012, A&A, 548, A126
Minchev I., Martig M., Streich D., Scannapieco C., de Jong R. S., Steinmetz M., 2015, ApJ, 804, L9
Ocvirk P., Pichon C., Lançon A., Thiébaut E., 2006a, MNRAS, 365, 46
Ocvirk P., Pichon C., Lançon A., Thiébaut E., 2006b, MNRAS, 365, 74
Pérez E. et al., 2013, ApJ, 764, L1
Pohlen M., Trujillo I., 2006, A&A, 454, 759
Radburn-Smith D. J. et al., 2012, ApJ, 753, 138
Roediger J. C., Courteau S., Sánchez-Blázquez P., McDonald M., 2012, ApJ, 758, 41
Roškar R., Debattista V. P., Stinson G. S., Quinn T. R., Kaufmann T., Wadsley J., 2008, ApJ, 675, L65
Ruiz-Lara T. et al., 2015, A&A, 583, A60
Sánchez S. F. et al., 2012a, A&A, 538, A8
Sánchez S. F. et al., 2012b, A&A, 546, A2
Sánchez S. F. et al., 2014, A&A, 563, A49
Sánchez-Blázquez P., Courty S., Gibson B. K., Brook C. B., 2009, MNRAS, 398, 591
Sánchez-Blázquez P., Ocvirk P., Gibson B. K., Pérez I., Peletier R. F., 2011, MNRAS, 415, 709
Sánchez-Blázquez P. et al., 2014, A&A, 570, A6
Sarzi M. et al., 2006, MNRAS, 366, 1151
Schaye J., 2004, ApJ, 609, 667
Sellwood J. A., Binney J. J., 2002, MNRAS, 336, 785
van den Bosch F. C., 2001, MNRAS, 327, 1334
van der Kruit P. C., 1987, A&A, 173, 59
Vazdekis A., Sánchez-Blázquez P., Falcón-Barroso J., Cenarro A. J., Beasley M. A., Cardiel N., Gorgas J., Peletier R. F., 2010, MNRAS, 404, 1639
Walcher C. J. et al., 2014, A&A, 569, A1
Yoachim P., Roškar R., Debattista V. P., 2012, ApJ, 752, 97
Younger J. D., Cox T. J., Seth A. C., Hernquist L., 2007, ApJ, 670, 269
Zhang H.-X., Hunter D. A., Elmegreen B. G., Gao Y., Schruba A., 2012, AJ, 143, 47
Zheng Z. et al., 2015, ApJ, 800, 120

[1]*Departamento de Física Teórica y del Cosmos, Universidad de Granada, Campus de Fuentenueva, E-18071 Granada, Spain*
[2]*Instituto Carlos I de Física Teórica y computacional, Universidad de Granada, E-18071 Granada, Spain*
[3]*Departamento de Física Teórica, Universidad Autónoma de Madrid, E-28049 Cantoblanco, Spain*
[4]*School of Physics and Astronomy, University of St Andrews, SUPA, North Haugh, KY16 9SS St Andrews, UK*
[5]*Kapteyn Astronomical Institute, University of Groningen, PO Box 800, NL-9700 AV Groningen, the Netherlands*
[6]*Instituto de Astrofísica de Canarias, Calle Vía Láctea s/n, E-38205 La Laguna, Tenerife, Spain*
[7]*Departamento de Astrofísica, Universidad de La Laguna, E-38200 La Laguna, Tenerife, Spain*
[8]*Instituto de Astrofísica de Andalucía (CSIC), Glorieta de la Astronomía s/n, Aptdo. 3004, E-18080 Granada, Spain*
[9]*Instituto de Astronomía, Universidad Nacional Autónoma de México, A.P. 70-264, 04510 México D.F., Mexico*
[10]*Millennium Institute of Astrophysics, Santiago, Chile*
[11]*Departamento de Astronomía, Universidad de Chile, Camino El Observatorio 1515, Las Condes, Santiago, Chile*
[12]*European Southern Observatory (ESO), Karl-Schwarzschild-Str. 2, D-85748 Garching b. München, Germany*
[13]*Australian Astronomical Observatory, PO Box 915, North Ryde, NSW 1670, Australia*
[14]*Department of Physics and Astronomy, Macquarie University, NSW 2109, Australia*
[15]*CEI Campus Moncloa, UCM-UPM, Departamento de Astrofśica y CC. de la Atmósfera, Facultad de CC. Físicas, Universidad Complutense de Madrid, Avda. Complutense s/n, E-28040 Madrid, Spain*
[16]*Department of Physics, Institute for Astronomy, ETH Zürich, CH-8093 Zürich, Switzerland*
[17]*Observatorio Astronómico, Laprida 854, X5000BGR, Córdoba, Argentina*
[18]*Consejo de Investigaciones Científicas y Técnicas de la República Argentina, Avda. Rivadavia 1917, C1033AAJ, CABA, Argentina*
[19]*Instituto de Astrofísica e Ciências do Espaço, Universidade do Porto, CAUP, Rua das Estrelas, P-4150-762 Porto, Portugal*
[20]*Max Planck Institute for Astronomy, Königstuhl 17, D-69117 Heidelberg, Germany*
[21]*Leibniz-Institude für Astrophysik Potsdam (AIP), An der Sternwarte 16, D-14482 Potsdam, Germany*
[22]*INAF - Osservatorio Astrofisico di Arcetri, Largo Enrico Fermi 5, I-50125 Firenze, Italy*

This paper has been typeset from a TEX/LATEX file prepared by the author.